

SUBSTRATE AND ANNEALING EFFECTS ON THE PULSED-LASER DEPOSITED TiO₂ THIN FILMS

L. S. Hsu, D. Luca^{a*}

Department of Physics, National Chang-Hua University of Education, Chang-Hua 50058, Taiwan, Republic of China

We report on the optimized preparation and characterization of pulsed-laser deposited anatase TiO₂ thin films on single-crystal substrates at a substrate temperature of 500 °C and under 0.02-20 mTorr O₂. The effect of *ex-situ* annealing of TiO₂ thin films under 1 atm O₂ was investigated as a function of temperature. Despite thermodynamically unstable, the anatase TiO₂ thin films are successfully prepared on the LaAlO₃, SiO₂, and SrTiO₃ substrates. Film morphology, composition, and structure were investigated by various techniques. Wavelength dependence of the refractive index and absorption coefficient in the UV-VIS-near IR regions were inferred from spectro-photometry data. The wettability of the TiO₂ films was evaluated from static contact angle measurements. The experimental results are interpreted in terms of the effects of amorphous-to-crystalline phase transition and subsequent oxidation of the annealed films.

(Received June 26, 2003; accepted August 21, 2003)

Keywords: Anatase TiO₂ thin films, Pulsed-laser deposition, Raman shift, Optical transmittance, Contact angle

1. Introduction

Bulk crystalline TiO₂ has three crystallographic polymorphs: anatase, brookite, and rutile [1]. The former two structures are metastable below 700 °C, while rutile structure is thermodynamically stable up to the melting point. Amorphous and rutile TiO₂ thin films have many applications in microelectronics, microwave technique, optics, and medicine [2-4], and the anatase TiO₂ phase possesses the peculiar photo-catalytic property [5,6,7]. Several fabrication methods of TiO₂ thin films have been used, most of them based on rf and dc reactive magnetron sputtering [5,6,8] and plasma-enhanced chemical vapor deposition [9]. On the other hand, a significant effort has been made during the recent years to improve the quality of the TiO₂ films prepared by pulsed-laser deposition (PLD). PLD is a simple and relatively low-cost method to grow oxide films with excellent composition match between the deposited film and the ablated target. The PLD-prepared TiO₂ films are usually amorphous when the substrate temperature is below 300 °C. In many applications, deposition of crystal-grade anatase or rutile TiO₂ films is required. Simplifying the preparation procedures to grow high-quality crystalline TiO₂ films can be achieved by appropriate choices of substrate type, substrate temperature, deposition geometry, process gas pressure, and *ex-situ* annealing condition. The large-size aggregate particles often found in the PLD-deposited TiO₂ films can be eliminated by careful adjustment of laser energy, buffer gas pressure, and using mechanical means for particle filtering [10].

In this paper, we report on preparation and characterization of crystalline TiO₂ thin films grown by PLD [11]. These films were deposited on various single-crystal substrates: (100) Si, (100) SiO₂, (100) MgO, (100) SrTiO₃ (STO), (100) LaAlO₃ (LAO) and (100) yttria-stabilized zirconia (YSZ). Post-deposition annealing was used to increase crystallinity, optical, and wetting properties of the prepared films. Film characterization has performed by secondary-ion mass spectrometry (SIMS),

^a On leave from the Faculty of Physics, Al. I. Cuza University, Iasi, Romania

* Corresponding author: dluca@cc.ncue.edu.tw

x-ray diffraction (XRD), atomic force microscopy (AFM), scanning electron microscopy (SEM), energy dispersive x-ray spectroscopy (EDX), UV-VIS-NIR spectro-photometry, and contact-angle measurement.

2. Experimental

TiO₂ thin films were grown in a PLD vacuum chamber, in which a base pressure of 1×10^{-6} Torr could be routinely achieved by using a turbo-molecular pumping system. A gas sampling system built around a Stanford Research Systems residual-gas analyzer was used for monitoring the gas composition inside the chamber. The O₂ gas pressure was varied between 1×10^{-5} mTorr and 20 mTorr. A laser beam originating from a Lambda Physik COMPex 102 KrF excimer laser ($\lambda = 248$ nm, 20 ns pulse duration, and 5 Hz repetition rate) was focused onto the target at an incident angle of 45°. In all deposition experiments the films were prepared under 6000 laser shots, 100 mJ each, focused on a 3.5×0.5 mm² of the ablated target. This laser energy was chosen to minimize the occurrence of droplets or cluster/aggregates within the films. The target was a powder-sintered (1400 °C, 4 h) TiO₂ pellet, which was fastened on a rotating substrate to constantly move the ablation spot to fresh site. The target-to-substrate distance was kept at 35 mm.

TiO₂ films were grown on different substrates mentioned above. Before deposition, the substrates were sonicated for 15 min in acetone, then rinsed and soaked. Four series of samples were deposited under oxygen pressures of 20, 7, 1, and 0.02 mTorr, all at a substrate temperature of 500 °C. Each sample was sequentially *ex-situ* post-annealed for 1h at 600, 650, 700, and 900 °C under 1 atm of pure O₂. The film structure was determined by XRD using the Fe K_α radiation ($\lambda = 1.93604$ Å) of an SCINTAG DMS 2000 equipment. Complementary information concerning film structure was derived from Raman spectra, which were acquired using a SPEX 1403 0.85m double spectrometer with an Ar⁺ laser ($\lambda = 488$ nm) as excitation source. Film microstructure and composition were determined from SEM and EDX measurements performed on a Hitachi S3000N SEM equipped with a Horiba electron microprobe. AFM measurements were done using a Quesant Q-Scope 350CL AFM in different operation modes. Depth profiles of elemental distribution in the films were measured with a Cameca IMS-4F SIMS using a 230 nA, 8 keV O₂⁺ primary beam. Spectro-photometric measurements were done using a UV-VIS-NIR spectrophotometer (JASCO, V570). Measurements of static contact angle between de-ionized water and TiO₂ films were performed in ambient temperature (60 % humidity) using the sessile drop method under receding drop condition. UV irradiation of the TiO₂ films was done with the unfocussed excimer laser at energy density of 18 mJ/cm² per pulse. Contact angle was monitored as a function of UV irradiation time until a saturation state was reached. Afterwards, samples were kept in a dark place and the recovery evolution of the contact angle was monitored for 72 h.

3. Results and discussion

3.1. Film morphology and composition

Figs. 1 (a) and (b) show AFM the images of two TiO₂ samples deposited on Si substrate under oxygen pressure of 1.6 and 20 mTorr, respectively. As seen in Fig. 1(a), the as-deposited TiO₂ thin films featured a smooth surface with no grain boundary and few droplets and cluster/aggregates of sub-micron size. The surface roughness of the TiO₂ thin films increases with film thickness, annealing temperature, and annealing time. Other AFM measurements showed that surface roughness increased more than 30 times when oxygen pressure increased from 1.6 to 20 mTorr.

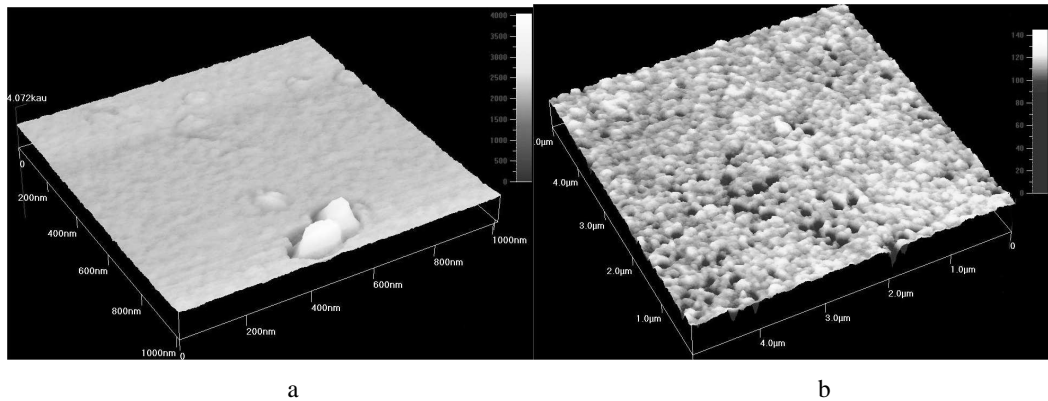


Fig. 1. Phase-mode AFM images of two TiO₂ thin films deposited on Si under (a) 1.6 mTorr and (b) 20 mTorr oxygen pressure.

A typical cross-section/surface SEM image of a TiO₂ film under oxygen pressure of 7 mTorr is shown in Fig. 2. Few droplets and cluster/aggregate occur on a smooth surface. Other cross-sectional SEM images showed such clusters embedded within the film. The occurrence of large-size particles in our films is due to the incomplete elimination of crater-like features on the target surface, which is caused by ultra-rapid laser evaporation of target material. The EDX measurements show that the O/Ti atomic ratio in the surface region of the film increases from 15% for the samples deposited at 0.02 mTorr until 53% for the films grown at 20 mTorr and remains practically constant as pressure increases. Films deposited at lower pressures are oxygen-deficient and tend to become stoichiometric when deposited under higher oxygen pressures. It is estimated that a significant fraction of the oxygen atoms are bounded to Si, since no initial substrate preparation was done in order to remove the SiO₂ layer. Therefore, annealing was done to diminish oxygen vacancies and obtain stoichiometric films.

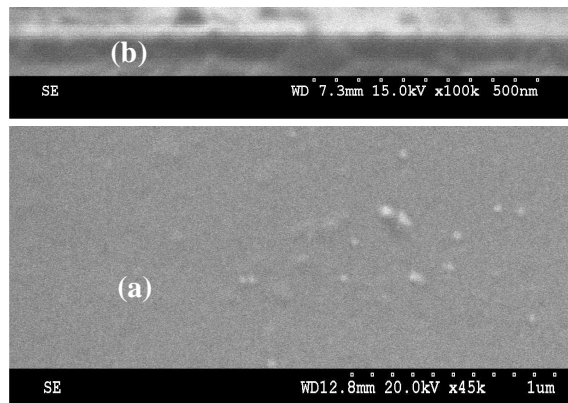


Fig. 2. (a) Cross-section and (b) surface SEM images of a TiO₂ thin film grown on Si.

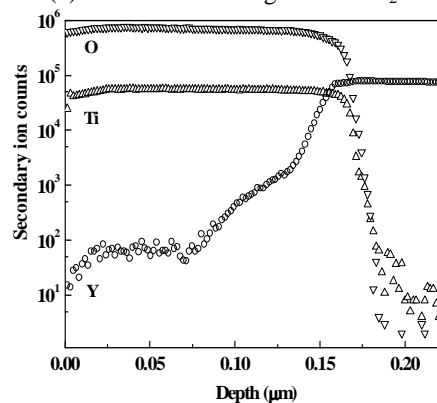


Fig. 3. A SIMS depth profile of a TiO₂ film grown on YSZ.

Fig. 3 shows a SIMS depth profile of a TiO₂ film deposited on YSZ at 20 mTorr O₂. Very sharp interface (~25 nm) is observed and almost no interface mixing is present between TiO₂ film and YSZ substrate. A good film adherence was noticed by scratch and stick-tape method. From both SIMS depth-profiling and cross-sectional SEM measurements, the thickness of the TiO₂ films ranges between 120 and 160 nm as a function of oxygen pressure. This spread is due to gas scattering of the ablated particles under the condition that the plasma plume size is significantly smaller than the target-to-substrate distance. The SIMS data suggest quite uniform distribution of elemental composition in depth for the TiO₂ films.

3.2. Film structure

Fig. 4 shows the XRD pattern of a TiO₂ thin film grown on the Si under 7 mTorr O₂ for the samples as-deposited and after successive annealing at temperatures between 600 and 1000 °C. For reference, the XRD pattern of the ablated pellet is also shown in Fig. 4. The XRD pattern of the as-deposited sample shows a very weak (101) TiO₂ anatase peak at 31.9°. No rutile or brookite peak is observed. All films deposited at 500 °C on Si look amorphous from the XRD data. A large anatase diffraction peak occurs after annealing at 600 °C under 1 atm pressure of O₂. There is also a tiny (110) rutile peak appeared at 34.7°. Subsequent annealing under the same O₂ pressure but at increasing temperatures showed a gradual increase of the rutile phase and a diminishing of the anatase phase. The (101) anatase peak vanishes after annealing at 1000 °C.

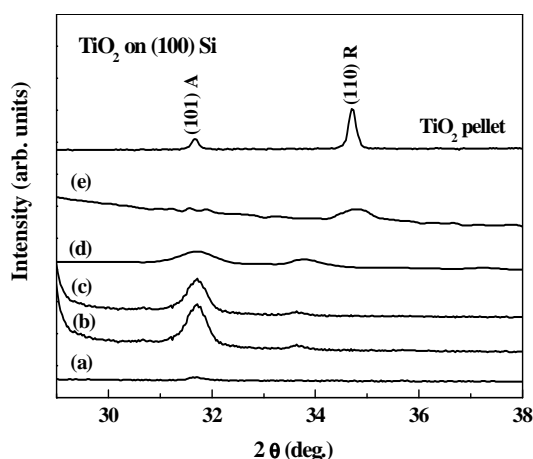


Fig. 4. XRD patterns of (a) an as-deposited TiO₂ thin film on Si and after successive annealing at (b) 600 °C, (c) 650 °C, (d) 750 °C, and (e) 1000 °C.

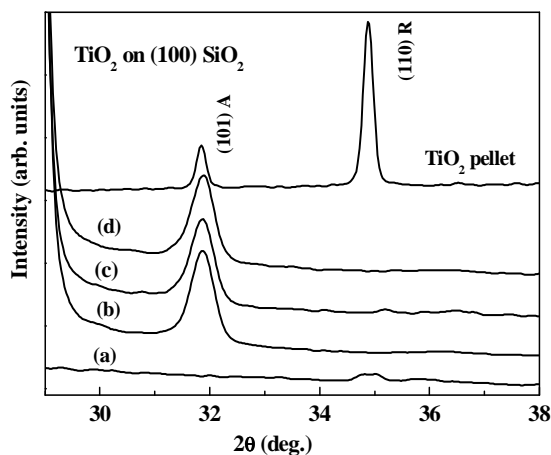


Fig. 5. XRD patterns of (a) an as-deposited TiO₂ thin film on SiO₂ and after successive annealing at (b) 600 °C, (c) 750 °C and (d) 1000 °C.

As shown in Fig. 5, the XRD patterns of the as-deposited TiO₂ thin film on quartz display amorphous and rutile phases. The XRD pattern of the TiO₂ target is also shown. The XRD patterns change dramatically after annealing at 600 °C, when a (101) anatase narrow peak occurs. The subsequent annealing at higher temperatures results in a slight decrease in the anatase peak height and an increase in the peak width. We also observed pure anatase phase for the TiO₂ films deposited on the LAO substrate and after annealing to the highest temperature. Unfortunately, in this latter case, the (101) TiO₂ anatase peak overlaps with a large substrate peak. Thus, deconvolution is necessary to monitor the evolution of the anatase phase. In the case of the STO substrate, the (101) TiO₂ anatase peak is completely hidden by a huge substrate peak in the XRD patterns. For STO and LAO substrates, the amorphous-to-anatase phase transformation can be observed by using the Raman scattering as will be shown below. We suspected that our films grown on STO substrates are anatase phase, too. A large amount of amorphous phase is observed in TiO₂ films deposited on the MgO

substrate. This amorphous phase transforms into a mixture of rutile and anatase phases after annealing in oxygen.

The Raman spectra provide information concerning the microstructure of the TiO₂ films. The Raman spectra also reveal the crystalline ordering with an information volume extending only over several unit cells. As is well known, the increase in peak height and the diminishing of the full-width at half-maximum of Raman peaks are due to diminishing of the lattice imperfection.

Fig. 6 shows the Raman spectra of a TiO₂ film deposited at 500 °C on an STO substrate under oxygen pressure of 7 mTorr. A clearly defined anatase E_{1g} Raman peak occurs at 145.0 cm⁻¹ of an as-deposited TiO₂ film. After oxygen annealing, the intensity of the peak increased, the peak width decreased. This Raman peak also appeared slightly shifted (0.7 cm⁻¹) towards smaller wavenumbers. This blue shift after annealing is connected with oxygen deficiency and non-stoichiometry in the as-deposited films. Additional asymmetric broadening and blue shift of the main anatase Raman peak may be correlated with the increase in crystallite sizes in our films [12]. Surprisingly, Raman spectra showed the occurrence of anatase-type nano-crystallites even for the as-deposited films grown on Si, which looked amorphous from XRD data.

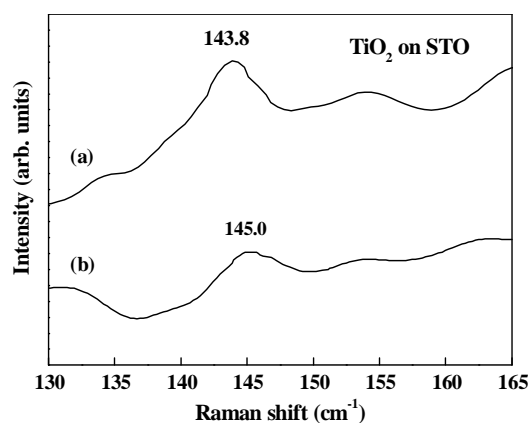


Fig. 6. Raman spectra of a TiO₂ thin film grown on STO for (a) as-deposited film and (b) annealed at 600 °C for 1h.

3.3. Optical properties

Fig. 7 shows the optical transmittance spectra of a TiO₂ thin film deposited on transparent quartz and annealed at 600 and 650 °C. The progressive annealing results in an increase of overall film transmittance, which is associated with changes in the visual aspect of the films. TiO₂ thin films are dark gray after deposition, become transparent after annealing at 600 °C, and then turn light gray after annealing at 1000 °C. The increase in the overall optical transmittance was previously observed for sputtered anatase-rutile mixture of TiO₂ polycrystalline thin films [8]. This is the result of the decrease of oxygen vacancy concentration in the films through annealing in oxygen atmosphere. This conclusion is also consistent with the EDX data, which indicate the presence of Ti sub-oxides in the as-deposited films, followed by an increase of the oxygen content after annealing in O₂ atmosphere.

The second effect of annealing is the shift of the spectrum in the UV region towards lower wavelength. As pointed out by our XRD and Raman data, annealing at 600 and 650 °C results in an amorphous-to-anatase phase transition. The blue shift in the transmittance spectra was previously observed in the sputtered films and ascribed to annealing-induced amorphous-to-anatase and anatase-to-rutile phase transformations [8]. Sputtered crystalline TiO₂ films are usually mixtures of rutile and anatase phases when deposited at temperatures between 300 and 600 °C. In contrast, we observe the occurrence of the blue shift in pure anatase TiO₂ films deposited by PLD after annealing at temperatures below 750 °C.

3.4. Film wettability

Fig. 8 shows the evolution of the contact angle during irradiation and recovery of an as-deposited TiO₂ film on STO substrate under 0.02 mTorr O₂. The contact angle drops to less than 50% of the initial value after 600 laser shots, which corresponds to UV radiation energy of 10.7 J. A saturation value of 29° is reached after 1200 laser shots. As shown in Table 1, similar behavior of the evolution of the contact angle was observed for TiO₂ films deposited on various substrates and O₂ pressures. The as-deposited non-irradiated amorphous samples grown on MgO and SiO₂ substrates have the highest contact-angle values (84° and 77°, respectively). The anatase TiO₂ films deposited on the STO and LAO substrates and annealed at 600 °C under O₂ show the sharpest drop in contact angle and smallest final contact angles (23° and 21°, respectively) after UV irradiation. We suspect that this effect is due to the photo-induced reactions on the surface of the anatase film. The contact angle of the samples kept in darkness increases in the initial stage, and saturates after characteristic time of the order of tens of hours. When TiO₂ films have anatase structure and large grain size, contact angles as low as 10° can be achieved after annealing the films at 700 °C for 1 h. Low contact angle means good wettability, which can also be achieved when high surface roughness is present. Recovery of the contact angle is a strong proof of the photocatalytic behavior of our TiO₂ thin films.

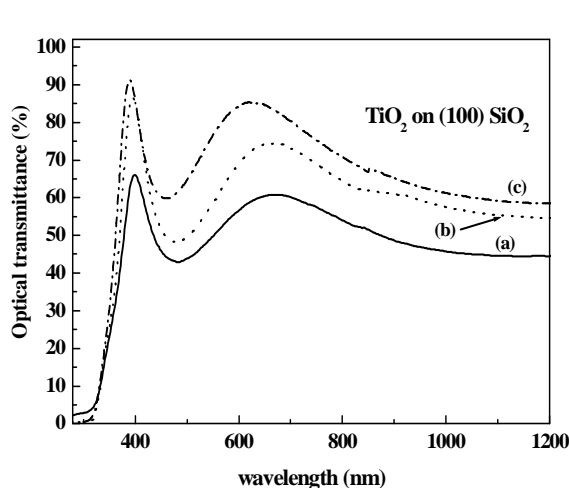


Fig. 7. Transmittance spectra of a TiO₂ thin film for (a) as-deposited, (b) annealed at 600 °C, and (c) annealed at 650 °C.

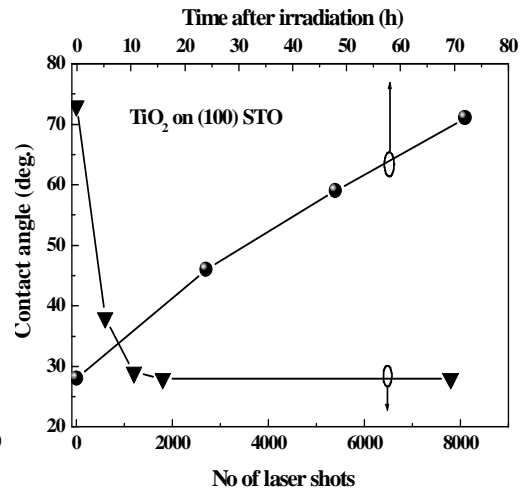


Fig. 8. Contact angle of a TiO₂ thin film as a function of number of laser shots during irradiation and as a function of time after post-irradiation.

Table 1. Contact angle, θ_c , between de-ionized water and eight TiO₂ thin films deposited on five substrates under three oxygen pressures (p_{O_2}).

Substrate	p_{O_2} (mTorr)	θ_c (deg.)				
		non-irradiated film	after 1500 shots	after 24 h	after 48 h	after 72 h
STO	1.6	71	36	69	70	70
STO*	1.6	54	23	50	51	52
MgO	1.6	84	60	62	67	72
LAO*	1.6	44	17	31	35	38
SiO ₂	7	77	45	58	69	74
Si	7	72	55	63	69	71
Si*	7	56	24	45	54	56
Si*	20	51	21	38	47	49

* Sample annealed for 1h under 1 atm of O₂.

4. Conclusions

We have prepared and investigated the morphological, structural, and optical properties of PLD-deposited anatase TiO₂ thin films. High-quality photo-catalytic poly-crystalline TiO₂ anatase films can be grown by PLD at moderate substrate temperature under oxygen pressures between 1 and 20 mTorr and followed by annealing in 1 atm O₂ at 600-650 °C for 1 h. A large amount of amorphous phase was found in the as-deposited films. A small amount of TiO₂ anatase phase was identified in the as-deposited films on Si and LAO substrates. Raman data showed that nano-crystallization occurred in the films deposited on SiO₂ and MgO substrates, for which the XRD patterns displayed the lack of crystallinity. The enhanced crystallinity in films deposited on STO and LAO was ascribed to good lattice match between the TiO₂ anatase phase and these substrates. The structure data correlate well with the optical and contact-angle results. Films deposited at low pressures are oxygen-deficient and become stoichiometric after subsequent annealing in oxygen. Surface roughness is an additional factor for increased film hydrophilicity.

Acknowledgements

We thank Y.-T. Lee and Y. C. Chi for help in Raman and SEM measurements, respectively. This work has been sponsored by the National Science Council, Taiwan, Republic of China under Grants NSC91-2112-M-018-007 and NSC 92-2811-M-018-001.

References

- [1] A. K. Sharma, R. K. Tareja, U. Willer, W. Schade, *Appl. Surf. Sci.* **206**, 137 (2003).
- [2] N. J. Parker, P. Kharel, J. R. Powel, P. A. Smith, P. D. Evans, A. Porch, *IEEE Trans. Appl. Supercond.* **7**, 1928 (1999).
- [3] H. Kumagai, K. Toyoda, K. Kobayashi, M. Obara, Y. Iimura, *Appl. Phys. Lett.* **70**, 2338 (1997).
- [4] J. Li, *Biomaterials* **14**, 229 (1993).
- [5] P. Zeman, S. Takabayashi, *J. Vac. Sci. Technol.* **A20** (2), 388 (2002).
- [6] K. Okimura, A. Shibata, *Jpn. J. Appl. Phys.* **36**, 313 (1997).
- [7] L. Sirghi, T. Aoki, Y. Hatanaka, *Thin Solid Films* **422**, 55 (2002).
- [8] M. H. Suhail, G. Moran Rao, S. Mohan, *J. Appl. Phys.* **71**(3), 1421 (1991).
- [9] H.-K. Ha, M. Yoshimoto, H. Koinuma, *Appl. Phys. Lett.* **68** (21), 2965 (1996).
- [10] L.-C. Chen, *Particulates Generated by Pulsed Laser Ablation in Pulsed Laser Deposition of Thin Films*, D. B. Chrisey and G. K. Hubler (eds), John Wiley, NY, 1994, p. 190.
- [11] D. Luca, L. S. Hsu, *J. Optoelectron. Adv. Mater. Adv.* **5**(4), 785 (2003).
- [12] W. F. Zhang, Y. L. Le, M. S. Zhang, Z. Yin, Q. Chen, *J. Phys. D: Appl. Phys.* **33**, 912 (2000).